Two Novel Transition-Metal Phosphite Compounds with 4-, 6- and 12-Membered Rings: Hydrothermal Syntheses, Crystal Structures and Magnetic Properties of $Na_2[M(HPO_3)_2]$ (M = Fe, Co)

Wei Liu,[a] Hao-Hong Chen,[a] Xin-Xin Yang,[a] and Jing-Tai Zhao*[a]

Keywords: Synthesis / Structure / Cobalt / Iron / Phosphites / Magnetic properties

Two transition-metal phosphites, $Na_2[M(HPO_3)_2]$ (M = Fe, Co) with a new structure type have been synthesised under mild hydrothermal conditions and the solid-state structures have been elucidated by single-crystal X-ray diffraction studies. The structures are of a new type with the following data: orthorhombic, *Pnma*, a = 12.169(4), b = 5.441(2) and c = 9.146(3) Å for the iron species **1** and a = 12.091(3), b = 5.400(4) and c = 9.115(2) Å for the cobalt compound **2**, with Z = 4. The crystal structures of these compounds are isotypic and built up from a 3D open framework with 4-, 6- and 12-membered polyhedral rings of vertex-linked MO_6 and HPO_3 building units. The inorganic frameworks contains 12-membered ring channel systems in which the sodium ions are located. The topology of this structure type is remarkably similar to that of the aeschynite $CaTa_2O_6$ with much larger channels. Magnetic measurements of $Na_2[Co(HPO_3)_2]$ show different magnetic features in the low-temperature (5–30 K) and high-temperature ranges (100–320 K) suggesting the possible existence of a complex magnetic structure. Antiferromagnetic ordering can be observed as a broadened cusp in χ^{-1} at θ = 2.6 K. For $Na_2[Fe(HPO_3)_2]$, the magnetic behavior follows the Curie–Weiss law with μ_{eff} = 5.41 μ_B, fitted for 100–320 K.

Introduction

Transtion-metal phosphates with open-framework structures are of great interest from both an industrial and an academic point of view due to their applications as catalysts, ion-exchangers and molecular sieves.[1] Although attention has focused initially on the phosphates of aluminium and gallium because of their structural similarities with zeolites and clays, numerous open-framework transition-metal phosphates with novel properties are also known.[2–17] Besides, in the past few years, considerable efforts have been devoted to exploratory work on the possibilities of incorporating the phosphorus atom as a pseudo-pyramidal HPO_3^{2-} hydrogen phosphite group into extended structures and these studies have yielded a structurally diverse range of transition-metal phosphites, e.g. $(VO)(HPO_3)(H_2O)_5$ with isolated single chains,[18] $ZnCa(HPO_3)_2(H_2O)_2$,[19] $Fe(HPO_3H)_3$,[20] $M(HPO_3)(H_2O)$ (M = Co, Ni)[21] and $(NH_4)_2Zn_5(HPO_3)_6(H_2O)_4$[22] with layered structures as well as $NaM(H_2PO_3)_3(H_2O)$ (M = Mn, Co),[23] $[Zn_2(H_2O)_4](HPO_3)_2(H_2O)$,[24] $Na_2Zn_3(HPO_3)_4$[24] and $M_{11}(HPO_3)_8(OH)_6$ (M = Co, Ni, Zn)[25] with 3D structures. A few examples of inorganic-organic hybrid phosphites with transition-metal elements (V, Cr, Co, Mn, Fe) have also been reported in the literature.[26–30] However, phosphites with transition-metal elements have not been studied widely when compared with the related phosphates. In order to further examine the structural chemistry of these types of materials containing the first series of transition elements, we synthesised two new transition-metal phosphites of formula $Na_2[M(PO_3H)_2]$ (M = Fe, Co). The crystal structures of these compounds and their magnetic properties are also reported in this paper.

[a] The State Key Laboratory of High Performance Ceramics and Superfine Microstructure, Shanghai Institute of Ceramics, Chinese Academy of Science,
Shanghai 200050, P. R. China
Fax: +86-21-52413122
E-mail: jtzhao@mail.sic.ac.cn

Results and Discussion

Synthesis

Reactions of phosphorous acid with the transition-metal salts in the presence of NaOH under mild hydrothermal conditions afforded two new isostructural complexes with 3D open-frameworks. According to experimental investigations, we noted that the pH value has a significant influence on the reaction products. To obtain information about the reactive process of $Na_2[M(HPO_3)_2]$ (M = Fe, Co), an in-depth study at various pH values was carried out. Different experiments were performed with the pH = 1.0, 3.0, 5.0, 7.0 and 9.0 but all other conditions were kept constant. The study of the final products by X-ray powder diffraction measurements revealed that when the pH ≤ 5.0, the reactions lead to an unknown powder for $Na_2[Fe(HPO_3)_2]$ (**1**)

 DOI: 10.1002/ejic.200400644

and a known compound, $Co(PO_3H)\cdot H_2O$ (JCPDS: 44-1323) for $Na_2[Co(HPO_3)_2]$ (**2**) while with a pH > 5.0 the title compounds were isolated as pure phases (Scheme 1). When thinking about the synthesis of transition-metal derivatives of this low-oxidation-state phosphorous acid, it becomes necessary to consider the problems resulting from the hydrolytic processes of phosphorous acid which would be essentially controlled by the pH of the solution.[31] In this context, it becomes possible to understand the experimental results obtained when the syntheses of the title compounds were performed. Since the protons of the phosphorous acid are easily removed under alkaline conditions, the phosphorus atom is suitable for simultaneously binding to three M^{II} atoms to form the polyhedral network of alternating MO_6 and PO_3H units in the title compounds. On the contrary, with a decrease in the pH value, less protons from the phosphorous acid can be removed which correspondingly reduces the degree of coordination of the phosphorus atoms to the M^{II} atoms. Therefore, the cationic groups in the solution tend to aggregate themselves under suitable conditions, leading to the resultant cationic network in the final solid $Co(PO_3H)\cdot H_2O$. Similar results have also been reported by Marcos et al. in their synthetic process.[25] For example, they were also able to prepare $M(HPO_3)(H_2O)$ (M = Co, Ni, Zn) at low pH whereas by carrying out the synthesis at intermediate pH values, other compounds with a different structure type were obtained, namely $M_{11}(HPO_3)_8(OH)_6$ (M = Zn, Co, Ni). All the above observations indicate that the pH of the solution indeed plays a crucial role in the reactive process and mainly determines the stability ranges of the various compounds.

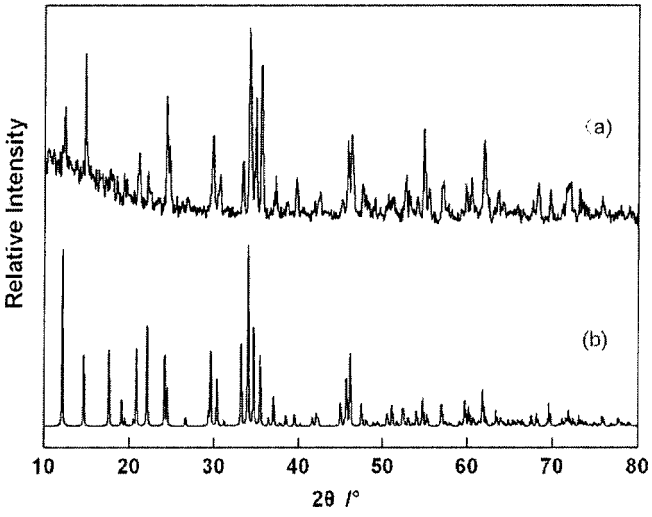

Scheme 1. Observed (a) and calculated (b) X-ray powder diffraction profiles for $Na_2[(CoPO_3H)_2]$

Crystal Structures of $Na_2[M(HPO_3)_2]$ (M = Fe and Co)

The crystal structures of the two isotypic compounds both contain a 3D anionic framework made from polyhedral linkages between MO_6 and HPO_3 units sharing common O-corners. Such connectivities between these units produce numerous six-membered rings which connect to each other by sharing common edges giving rise to an infinite honeycomb-like six-membered sheet in the *bc* plane [see Figure 1 (left)]. Pairs of phosphite groups are distributed between these sheets and bridge the sheets into the whole 3D open-framework. An offset between the sheets in the [001] direction destroys the formation of a six-membered ring channel system along the *a* axis [see Figure 1 (right)] but the 4- and 12-membered ring channel systems are distributed alternately in the structure along the *b* axis which is enclosed by the 4- and 6- membered ring walls [see Figure 2 (d)]. The shape of the 12-membered ring channel is close to rhombohedral with the largest length being 12.8 Å and the smallest being 6.8 Å. Therefore, the structures of the title compounds examined here can also be characterised by the presence of an infinite number of 4-, 6- and 12-membered polyhedral rings.

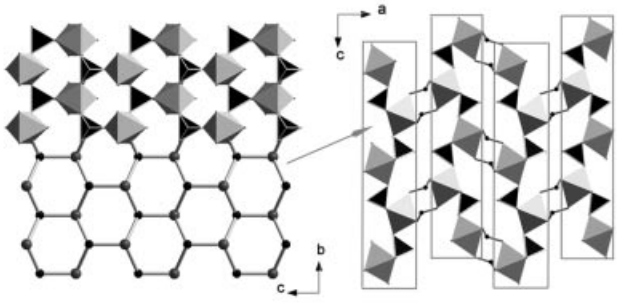

Figure 1. (left) The 6-membered ring polyhedral sheet in the *bc* plane constructed from alternating MO_6 and HPO_3 polyhedra. (right) The parallel stack of 6-membered ring sheets along the [010] direction showing the offset along the *c* axis between the sheets (MO_6, grey octahedron; PO_3H, dark tetrahedron; M atom, gray sphere; P atom, dark sphere).

More importantly, a detailed analysis of the structures allows the entire framework in each case to be described as an assembly of multiple ribbons running along the *b* axis. Such multiple ribbons are built up from two distinct types of single polyhedral ribbons: the linear chain possessing corner-shared four-membered rings [Figure 2(a)] and the ladders with edge-sharing four-membered rings [Figure 2 (b)]. The centred ladder interconnects with two neighbouring linear chains through edge sharing and forms a novel unbranched multiple-chain running along the *b* axis [Figure 2 (c)]. Such multiple-ribbons repeat themselves in parallel along the *c* axis in a zigzag-like manner with an angle of approximately 120° along the *a* axis [Figure 2 (d)], giving rise to a fish backbone-type arrangement in the *bc* plane. Such multiple-chains connect to each other through the M–O–P bridges to form the entire open-framework [Figure 2 (e)].

The guest Na^+ ions occupy the open spaces in the framework to maintain the structural stability and satisfy the charge balance. The $Na(1)^+$ ions are located in the twelve-membered ring channels and the $Na(2)^+$ ions occupy the centres of the six-membered rings, respectively (see Figure 3).

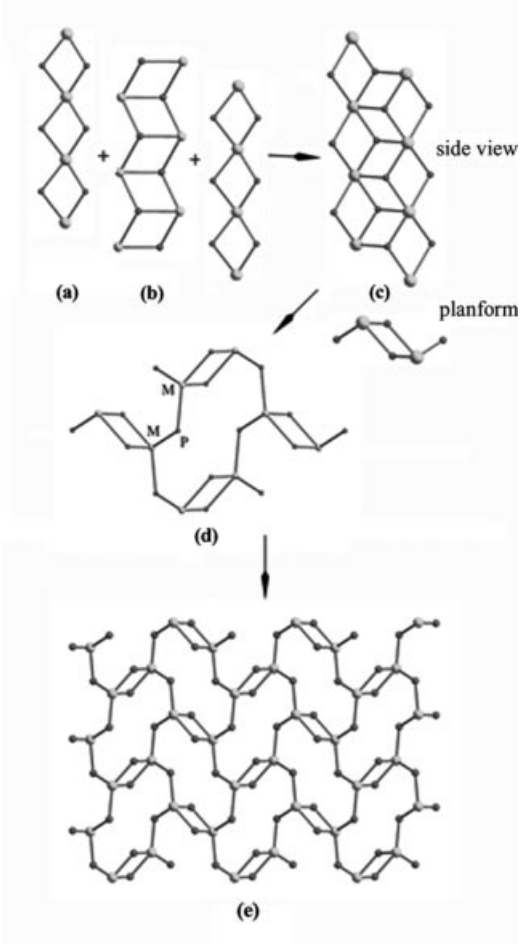

Figure 2. Schematic representation of the formation of the open-framework structure of $Na_2[M(HPO_3)_2]$ (M = Fe, Co). (a) The linear chain possessing corner-shared four-membered rings. (b) The ladders with edge-shared four-membered rings. (c) The loop-branched multiple ribbon. (d) The combination of four multiple ribbons to form a 12-membered ring via the M–O–P bridge. (e) The infinite 3D open-framework.

The topology of this structure is remarkably similar to that of the aeschynite $CaTa_2O_6$ (see Figure 4). According to the concept of scale chemistry,[32,33] the two structures can be considered as though they have the same walls (topology) but are built from different bricks (BUs). The latter has the double rows of TaO_6 octahedra as BUs, while the former has an upper analogue in which the BUs are the multiple ribbons made of corner-shared tetrahedra and octahedra. The *trans* corner linkage of the BUs givs rise to zigzag chains and Na^+ and Ca^{2+}cations are located in similarly oriented tunnels in these phosphites and in the aeschynite, respectively. The augmentation of the 4,6 net in the aeschynite structure largely increases the porosity of the structure. The channels (12.8 × 6.8 Å) in the title compounds are more expanded compared with those (7.67 × 4.93 Å) in the aeschynite as a result of the adoption of larger BUs which is consistent with the principle of scale chemistry, i.e. the larger the brick, the larger the pore. Thus, the present structural type, in addition to being a new member of the family of $CaTa_2O_6$, also demonstrates that many structures can readily be designed and preformed to basic topologies dictated by the shapes (triangle, square, tetrahedron, etc.) and connectivities of the structural building units.

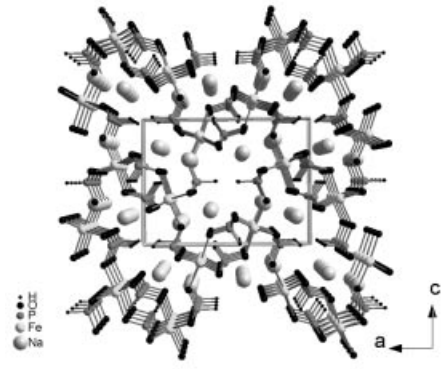

Figure 3. Structure of $Na_2[M(HPO_3)_2]$ (M = Fe, Co) along the [010] direction showing the 4-, 6-, and 12-membered polyhedral rings. The $Na(1)^+$ ions and $Na(2)^+$ ions are located in the channels and the centre of six-membered rings, respectively.

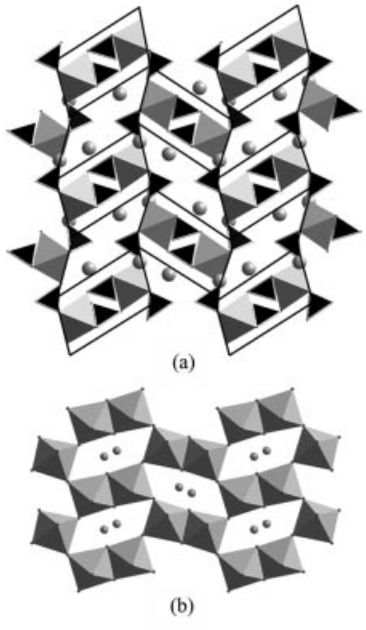

Figure 4. (a) The stacking of the multiple ribbons in $Na_2[M(HPO_3)_2]$ (M = Fe, Co) leading to a aeschynite-like framework. (b) The aeschynite ($CaTa_2O_6$) frameworks (Na atom, large gray sphere; Ca atom, small gray sphere).

For **1**, the FeO_6 octahedra have Fe–O distances in the range of 2.113(2)–2.171(2) Å whereas the *cis* and *trans* bond angles are in the ranges of 84.29(5)–96.04(4)° and 172.39(5)–174.64(7)°, respectively. For **2**, the Co–O distances vary from 2.079(2) Å to 2.147(2) Å and the *cis* and *trans* angles are in the ranges of 83.95(6)–95.77(4)° and 172.57(6)–174.99(7)°, respectively. These values are typical for Fe and Co in an octahedral oxygen environment. The

tetrahedral P atoms have P–O bond lengths in the ranges of 1.517(2)–1.522(2) Å for **1** and 1.518(2)–1.523(2) Å for **2** and the P–H distances vary between 1.31(7) and 1.46(5) Å [P(1)–H(2) = 1.31(7) Å, P(2)–H(1) = 1.396(1) Å in **1**; P(1)–H(2) = 1.34(7) Å, P(2)–H(1) = 1.46(5) Å in **2**]. These values are within the expected ranges. The Na cations reside in the irregular $Na(1)O_5$ and $Na(2)O_9$ environments and are coordinated to neighbouring phosphite groups by sharing common corners or edges. Additionally, Na(1) bonds to two hydrogen atoms of the HPO_3 groups with distances in the range of 2.608–2.872 Å. The Na–O bond lengths are quite diverse with Na(1)–O in the range of 2.36–2.41 Å and Na(2)–O in the range of 2.29–2.78 Å for compound **1**. For **2** the Na(1)–O distances are in the range of 2.35–2.39 Å and the Na(2)–O distances are in the range of 2.29–2.76 Å.

Magnetic Properties

Magnetic measurements of $Na_2[M(HPO_3)_2]$ (M = Fe, Co) were performed on crystalline samples in the temperature range of 1.8–320 K. The temperature dependence of the inverse molar magnetic susceptibilities, χ^{-1}, of compounds **1** and **2** in the range of 1.8–320 K are show in Figure 5 and Figure 6, respectively. Compound $Na_2[Co(HPO_3)_2]$ displays a magnetic susceptibility not obeying a simple Curie–Weiss law. If one separates the low- and the high-temperature ranges, the Curie–Weiss can be fit in the ranges of 100–320 K (HT) and 5–30 K (LT). For the low-temperature interval, an effective magnetic moment of 4.47 μ_B and θ = –21 K can be obtained. The effective magnetic moment per Co atom obtained from the LT fit is well within the range reported in the literature for octahedrally coordinated Co^{2+} ions (but also near to the value of 4.3 μ_B reported for Co^{3+}).[34] The effective magnetic moment for the high-temperature range is 5.30 μ_B which, while significantly larger than the spin-only value for spin S = centres (3.87 μ_B), indicates especially strong deviations of Co^{2+} from the spin-only value due to strong orbital contributions. A Weiss temperature θ = –50 K can be obtained, demonstrating dominant antiferromagnetic interactions between the magnetic centres at low temperature. The zero-field cooled samples measured under an external field of 100 Oe show a broadened cusp at 1 and 4 K in the χ^{-1} vs T curve, indicating antiferromagnetic ordering at low field [Figure 5 (inset)]. The different magnetic features at low and high temperatures indicate that the magnetic structure is complex. Similar magnetic properties can also be observed in $[Co_3(pyz)(HPO_4)_2F_2]$ and $[Co_3(4,4'\text{-bpy})(HPO_4)_2F_2]\cdot xH_2O$ (Figure 5).[35] For $Na_2[Fe(HPO_3)_2]$, the magnetic behaviour follows the Curie–Weiss law in the temperature range of 100–320 K (Figure 6). A fit in the range of 100–320 K gives an effective magnetic moment of 5.41 μ_B which is well within the range reported in the literature for octahedrally coordinated Fe^{2+} ions.[34] The asymptotic Curie–Weiss temperature θ is equal to –20.3 K, indicating antiferromagnetic exchange in compound **2**. There is possible magnetic ordering observed in fields as low as 1 kOe and above 1.8 K [Figure 6 (inset)].

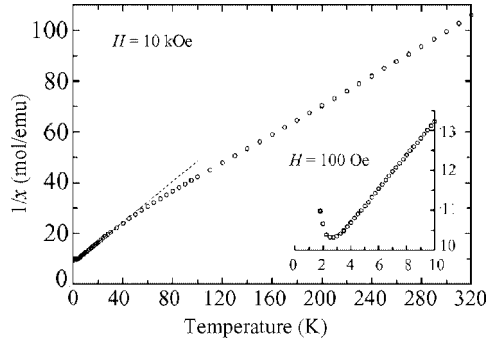

Figure 5. Inverse magnetic susceptibility (χ^{-1}, open circles) plotted as a function of temperature for powder samples of $Na_2[Co(HPO_3)_2]$. The inset shows the antiferromagnetic ordering at low temperature.

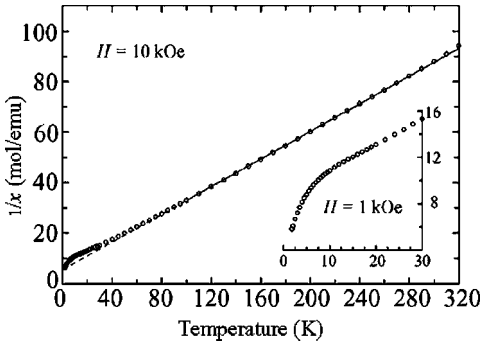

Figure 6. Inverse magnetic susceptibility (χ^{-1}, open circles) plotted as a function of temperature for powder samples of $Na_2[Fe(HPO_3)_2]$. The inset shows the possible magnetic ordering at low temperature.

Conclusions

Two new transition-metal phosphites with 4-, 6- and 12-membered polyhedral rings have been synthesised under mild hydrothermal conditions. Both of the compounds are constructed from strictly alternating MO_6 octahedra and HPO_3 tetrahedra through sharing the O-vertexes. Such connectivities between the units also form 4- and 12-membered ring channel systems in the framework structures in which the sodium ions are located. The topology of this structure is remarkably similar to that of the aeschynite $CaTa_2O_6$ and the augmentation of the BUs largely increases the channel size in the new compounds. Magnetic studies for $Na_2[Co(HPO_3)_2]$ show interesting features suggesting the possible existence of a complex magnetic structure at low temperature. For $Na_2[Fe(HPO_3)_2]$, the magnetic susceptibility obeys the Curie–Weiss law in the temperature range of 100–320 K with μ_{eff} = 5.41 μ_B which indicates Fe^{2+} character.

Table 1. Crystal structure refinement data for $Na_2[M(HPO_3)_2]$ (M = Fe, Co).

	1	2
Empirical formula	$H_2FeNa_2O_6P_2$	$H_2CoNa_2O_6P_2$
Formula weight	261.79	264.87
Wavelength [Å]	0.71073	0.71073
Crystal system	orthorhombic	orthorhombic
Space group	*Pnma* (no. 62)	*Pnma* (no. 62)
a [Å]	12.169(4)	12.091(3)
b [Å]	5.441(2)	5.400(4)
c [Å]	9.164(3)	9.115(2)
V [Å^3]	606.7(4)	595.1(3)
Z	4	4
D_c [g cm^{-3}]	2.866	2.956
μ(Mo-K_α) [mm^{-1}]	3.124	3.534
F(000)	512	516
θ range [°]	2.78–27.11	2.80–27.09
Total data	2760	2814
Unique data	727	724
Observe data	704	689
GOF on F^2	1.17	1.14
Final *R* indices	R_1[a] = 0.0224,	R_1[a] = 0.0210,
[$I > 2\sigma(I)$]	wR_2[b] = 0.0611	wR_2[b] = 0.0587
R indices	R_1[a] = 0.0230,	R_1[a] = 0.0222,
(all data)	wR_2[b] = 0.0615	wR_2[b] = 0.0592

[a] $R_1 = \Sigma||F_o| - |F_c||/\Sigma|F_o|$. [b] $wR_2 = \{\Sigma[w(F_o^2 - F_c^2)^2]/\Sigma[w(F_o^2)^2]\}^{1/2}$, $w = 1/[\sigma^2(F_o^2) + (0.0302P)^2 + 5.74P]$, $P = (F_o^2 + F_c^2)/3$.

Table 2. Selected bond lengths [Å] and angles [°] in $Na_2[Fe\text{-}(HPO_3)_2]$.

Fe(1)–O(4)	2.113(2)	Na(1)–O(1)[d]	2.363(2)
Fe(1)–O(1)	2.118(1)	Na(1)–O(2)[k]	2.386(3)
Fe(1)–O(1)[a]	2.118(1)	Na(1)–O(3)[k]	2.408(2)
Fe(1)–O(2)	2.130(2)	Na(1)–O(3)[l]	2.408(2)
Fe(1)–O(3)[a]	2.171(2)	Na(1)–H(1)	2.872(2)
Fe(1)–O(3)	2.171(2)	Na(1)–H(2)	2.620(2)
P(1)–O(4)[e]	1.517(2)	Na(2)–O(4)	2.291(2)
P(1)–O(1)	1.522(1)	Na(2)–O(1)[l]	2.657(2)
P(1)–O(1)[f]	1.522(1)	Na(2)–O(1)[n]	2.657(2)
P(1)–H(2)	1.31(7)	Na(2)–O(3)[n]	2.670(2)
P(2)–O(2)[h]	1.517(2)	Na(2)–O(3)[l]	2.670(2)
P(2)–O(3)[c]	1.517(2)	Na(2)–O(2)[k]	2.731(1)
P(2)–O(3)[h]	1.517(2)	Na(2)–O(2)[n]	2.731(1)
P(2)–H(1)	1.396(1)	Na(2)–O(3)[a]	2.784(2)
Na(1)–O(1)[j]	2.363(2)	Na(2)–O(3)	2.784(2)
O(4)–Fe(1)–O(1)[a]	95.98(4)	O(4)[e]–P(1)–O(1)[f]	113.22(6)
O(4)–Fe(1)–O(1)	95.98(4)	O(1)–P(1)–O(1)[f]	110.38(9)
O(1)[a]–Fe(1)–O(1)	87.97(6)	O(4)[e]–P(1)–H(2)	107.51(6)
O(4)–Fe(1)–O(2)	174.68(8)	O(1)–P(1)–H(2)	105.97(6)
O(1)[a]–Fe(1)–O(2)	87.84(4)	O(1)[f]–P(1)–H(2)	105.97(6)
O(1)–Fe(1)–O(2)	87.84(4)	O(3)[g]–P(2)–O(3)[c]	112.84(9)
O(4)–Fe(1)–O(3)	91.31(4)	O(3)[g]–P(2)–O(2)	112.20(7)
O(1)[a]–Fe(1)–O(3)	172.41(6)	O(3)[c]–P(2)–O(2)	112.20(7)
O(2)–Fe(1)–O(3)	84.75(4)	O(3)[g]–P(2)–H(1)	104.62(6)
O(1)–Fe(1)–O(3)	93.39(6)	O(3)[c]–P(2)–H(1)	104.62(6)
O(4)[e]–P(1)–O(1)	113.22(6)	O(2)–P(2)–H(1)	109.75(10)

[a] $x, -y + ½, z$. [b] $-x + ½, -y + 1, z + ½$. [c] $-x + ½, -y, z + ½$. [d] $-x, -y + 1, -z + 1$. [e] $-x, -y, -z + 1$. [f] $x, -y - ½, z$. [g] $-x + ½, y + ½, z + ½$. [h] $x, y, z + 1$. [i] $-x, y + ½, -z + 1$. [j] $-x + ½, -y + 1, z - ½$. [k] $-x + ½, y + ½, z - ½$. [l] $x, y + 1, z$. [m] $-x + ½, -y, z - ½$. [n] $x, y, z - 1$.

Table 3. Selected bond lengths [Å] and angles [°] in $Na_2[Co\text{-}(HPO_3)_2]$.

Co(1)–O(4)	2.080(2)	Na(1)–O(1)[d]	2.346(2)
Co(1)–O(1)[a]	2.094(2)	Na(1)–O(2)[k]	2.383(3)
Co(1)–O(1)	2.094(2)	Na(1)–O(3)[k]	2.390(2)
Co(1)–O(2)	2.099(2)	Na(1)–O(3)[l]	2.390(2)
Co(1)–O(3)	2.147(2)	Na(1)–H(1)	2.764(1)
Co(1)–O(3)[a]	2.147(2)	Na(1)–H(2)	2.608(2)
P(1)–O(4)[e]	1.518(2)	Na(2)–O(4)	2.287(2)
P(1)–O(1)[f]	1.523(2)	Na(2)–O(1)[l]	2.640(2)
P(1)–O(1)	1.523(2)	Na(2)–O(1)[n]	2.640(2)
P(1)–H(2)	1.34(7)	Na(2)–O(3)[n]	2.663(2)
P(2)–O(2)	1.516(2)	Na(2)–O(3)[l]	2.663(2)
P(2)–O(3)[d]	1.516(2)	Na(2)–O(2)[k]	2.709(1)
P(2)–O(3)[g]	1.516(2)	Na(2)–O(2)[n]	2.709(1)
P(2)–H(1)	1.46(5)	Na(2)–O(3)[a]	2.757(2)
Na(1)–O(1)[j]	2.346(2)	Na(2)–O(3)	2.757(2)
O(4)–Co(1)–O(1)[a]	95.71(5)	O(4)[e]–P(1)–O(1)[f]	113.04(6)
O(4)–Co(1)–O(1)	95.71(5)	O(1)P–(1)–O(1)[f]	110.24(9)
O(1)[a]–Co(1)–O(1)	87.72(6)	O(4)[e]–P(1)–H(2)	110.76(2)
O(4)–Co(1)–O(2)	175.05(8)	O(4)–P(1)–H(2)	104.55(6)
O(1)[a]–Co(1)–O(2)	87.85(4)	O(4)[f]–P(1)–H(2)	104.55(6)
O(1)–Co(1)–O(2)	87.85(4)	O(3)[h]–P(2)–O(3)[d]	112.87(9)
O(4)–Co(1)–O(3)	91.36(5)	O(3)[h]–P(2)–O(2)	112.24(7)
O(1)[a]–Co(1)–O(3)	172.62(6)	O(3)[d]–P(2)–O(2)	112.24(7)
O(2)–Co(1)–O(3)[a]	172.62(6)	O(3)[h]–P(2)–H(1)	104.88(6)
O(1)[a]–Co(1)–O(3)[a]	93.69(5)	O(3)[d]–P(2)–H(1)	104.88(6)
O(4)[e]–P(1)–O(1)	113.04(6)	O(2)–P(2)–H(1)	109.13(1)

[a] $x, -y + ½, z$. [b] $-x + ½, -y + 1, z + ½$. [c] $-x + ½, -y, z + ½$. [d] $-x, -y + 1, -z + 1$. [e] $-x, -y, -z + 1$. [f] $x, -y - ½, z$. [g] $-x + ½, y + ½, z + ½$. [h] $x, y, z + 1$. [i] $-x, y + ½, -z + 1$. [j] $-x + ½, -y + 1, z - ½$. [k] $-x + ½, y + ½, z - ½$. [l] $x, y + 1, z$. [m] $-x + ½, -y, z - ½$. [n] $x, y, z - 1$.

Experimental Section

General Remarks: All chemicals were obtained from commercial sources and used as received. The products were examined by powder X-ray diffraction (Rigaku D/max 2550V diffractometer, Cu-K_α radiation) in order to confirm their phase identity and purity. IR spectra were recorded with a Digilab-FTS-80 spectrophotometer from 4000 to 400 cm^{-1} using pressed KBr pellets of the samples. The magnetic susceptibility measurements were carried out with a SQUID magnetometer (Quantum-Design, MPMS XL-7) in the temperature range 1.8 K–320 K. The elemental analyses were performed with an ICP-AES (Vista AX ICP-AES) instrument.

$Na_2[Fe(HPO_3)_2]$ (1): $FeCl_2{\cdot}6H_2O$ (0.29 g), NaOH (0.125 g), H_3PO_3 (solid state, 2.56 g) and deionised water (15 mL) were mixed in a molar ratio of 2:2.5:25:667. A solution of $NH_3{\cdot}H_2O$ (40 wt.-%) was added to adjust the pH to 7.0 and the resultant solution was sealed in a 25-mL Teflon-lined stainless steel autoclave and heated under autogenous pressure at 433 K for 5 d. The resultant pink rod-like water-soluble crystals from the reaction were recovered by filtration, washed with ethanol and dried at room temperature. Yield: 0.258 g (80% based on $FeCl_2{\cdot}6H_2O$). $H_2FeNa_2O_6P_2$ (261.79): calcd. Fe 21.3, Na 17.6, P 23.6; found Fe 21.0, Na, 17.7, P 23.2. IR (KBr disk): $\tilde{\nu}$ = 2388 (m), 1170 (s), 1085 (s), 1025 (s), 998 (m), 591 (m), 501 (m) cm^{-1}.

$Na_2[Co(HPO_3)_2]$ (2): $CoCl_2{\cdot}6H_2O$ (0.3 g), NaOH (0.125 g), H_3PO_3 (solid state, 2.56 g) and deionised water (15 mL) were mixed in a molar ratio of 2:2.5:25:667. A solution of $NH_3{\cdot}H_2O$ (40 wt.-%) was added to adjust the pH to 7.0 and the resultant solution was sealed in a 25-mL Teflon-lined stainless steel autoclave and heated under autogenous pressure at 433 K for 5 d. The resultant pink rod-like water-soluble crystals from the reaction were recovered by filtration, washed with ethanol and dried at room temperature. Yield: 0.234 g (70% based on $CoCl_2{\cdot}6H_2O$). $H_2CoNa_2O_6P_2$ (264.87): calcd. Co 22.2, Na 17.4, P 23.7; found Co 21.7, Na 17.0, P 23.3.

IR (KBr disk): $\tilde{\nu}$ = 2383 (m), 1172 (s), 1095 (s), 1025 (s), 995 (m), 586 (m), 493 (m) cm^{-1}.

X-ray Crystallographic Study: Crystals of each compound were selected under a polarising microscope, glued to a thin glass fibre with cyanoacrylate (superglue) adhesive and inspected for singularity. Two of them with regular rod-like shapes were chosen ($0.40 \times 0.20 \times 0.20$ mm for **1** and $0.40 \times 0.15 \times 0.15$ mm for **2**) and data sets were collected with a Nonius Kappa CCD diffractometer (Mo-K_α radiation, λ = 0.71073 Å) at 293 K. For **1**, the θ range for data collection was from 2.79 to 27.12° and an absorption correction was applied with maximum and minimum transmission factors of 0.732 and 0.694, respectively. A total of 2760 reflections were collected with ω scans, yielding 727 unique observed reflections(R_{int} = 0.0233). For **2** the θ range for data collection was from 2.80 to 27.09° and an absorption correction was applied with maximum and minimum transmission factors of 0.702 and 0.661, respectively. A total of 2814 reflections were collected with ω scans, yielding 724 unique observed reflections(R_{int} = 0.0210). The intensity data were corrected for Lorentz and polarisationeffects. The structures were solved by direct methods and refined against $|F^2|$ with the aid of the SHELXTL-PLUS package.[36] The iron, cobalt, sodium, phosphorus and oxygen atoms were initially found and refined. The coordinates of hydrogen atoms on the phosphorus centres were obtained from difference Fourier maps. Additional information concerning the data collection and structure refinements is presented in Table 1 while selected interatomic distances are given in Table 2 and Table 3 for **1** and **2**, respectively. Further details of the crystal-structure investigations may be obtained from the Fachinformationszentrum Karlsruhe, 76344 Eggenstein-Leopoldshafen, Germany, on quoting the depository numbers CSD-414247 (**1**) and -414248 (**2**).

Acknowledgments

This work was supported by the Fund for Distinguished Young Scholars (No. 20025101) and a Key Project from the NNSF of China (No.50332050), State "863" project (No. 2002AA324070) and a fund from Shanghai Optical Science and Technology (No. 022261015).

[1] A. K. Cheetham, G. Ferey, T. Loiseau, *Angew. Chem. Int. Ed.* **1999**, *38*, 3268–3292.
[2] S. B. Harmon, S. C. Sevov, *Chem. Mater.* **1998**, *10*, 3020–3023.
[3] C. H. Lin, S. L. Wang, K. H. Lii, *J. Am. Chem. Soc.* **2001**, *123*, 4649–4650.
[4] G. Y. Yang, S. C. Sevov, *J. Am. Chem. Soc.* **1999**, *121*, 8389–8390.
[5] J. Do, R. P. Bontchev, A. J. Jacobson, *Inorg. Chem.* **2000**, *39*, 3230–3237.
[6] S. Fernandez, J. L. Mesa, J. L. Pizarro, L. Lezama, M. I. Arriortua, R. Olazcuaga, T. Rojo, *Chem. Mater.* **2000**, *12*, 2092–2098.
[7] W. Tong, G. G. Xia, Z. R. Tian, J. Liu, J. Cai, S. L. Suib, J. C. Hanson, *Chem. Mater.* **2002**, *14*, 615–620.
[8] S. S. Bao, L. M. Zheng, Y. J. Liu, W. Xu, S. H. Feng, *Inorg. Chem*. **2003**, *42*, 5037–5039.
[9] M. B. Korzenski, J. W. Kolis, *Inorg. Chem.* **2000**, *39*, 5663–5668.
[10] C. D. Peloux, A. Dolbecq, P. Mialane, J. Marrot, E. Rivière, F. Sécheresse, *Angew. Chem. Int. Ed.* **2001**, *40*, 2455–2457.
[11] A. Natarajan, K. Cheetham, *J. Solid State Chem.* **1998**, *140*, 435–439.
[12] S. Ekambaram, S. C. Sevov, *J. Mater. Chem.* **2000**, *10*, 2522–2525.
[13] K. H. Lii, Y. F.Huang, *Inorg. Chem.* **1999**, *38*, 1348–1350.
[14] X. Q. Wang, L. M. Liu, H. D. Cheng, K.Ross, A. J. Jacobson, *J. Mater. Chem.* **2000**, *10*, 1203–1208.
[15] S. Y. Mao, Y. X. Huang, Z. B. Wei, J. X. Mi, Z. L. Huang, J. T. Zhao, *J. Solid State Chem.* **2000**, *149*, 292–297.
[16] Y. P. Chiang, H. M. Kao, K. H. Lii, *J. Solid State Chem.* **2001**, *162*, 168–175.
[17] B. G. Shpeizer, X. Ouyang, J. M. Heising, A. Clearfield, *Chem. Mater.* **2001**, *13*, 2288–2296.
[18] B. S. Zakharova, A. B. Ilyukhin, N. N. Chudinova, *Zh. Neorg. Khim.* **1994**, *39*, 1443–1445.
[19] M. Shieh, K. J. Martin, P. J. Squattrito, A. Clearfield, *Inorg. Chem.* **1990**, *29*, 958–963.
[20] M. Sghyar, J. Durand, L. Cot, M. Rafiq, *Acta Crystallogr., Sect. C* **1991**, *47*, 2515–2517.
[21] F. Sapina, P. Gomez-Romero, M. D. Marcos, P. Amoros, R. Ibanez, D. Beltran, R. Navarro, C. Rillo, F. Lera, *Eur. J. Solid State Inorg. Chem.* **1989**, *26*, 603–617.
[22] L. E. Gordon, W. T. A. Harrison, *Acta Crystallogr., Sect. E* **2002**, *58*, i41–i43.
[22] R. Chmelikova, J. Loub, V. Petricek, *Acta Crystallogr., Sect. C* **1986**, *42*, 1281–1283.
[24] C. Y. Ortiz-Avila, P. J. Squattrito, M. Shieh, A. Clearfield, *Inorg. Chem.* **1989**, *28*, 2608–2615.
[25] M. D. Marcos, P. Amoros, A. Beltrh-Porter, R. Martinez-Mfiez, J. P. Attfields, *Chem. Mater.* **1993**, *5*, 121–128.
[26] S. Fernandez, J. L. Pizarro, J. L. Mesa, L. Lezama, M. I. Arriortua, R. Olazcuaga, T. Rojo, *Inorg. Chem.* **2001**, *40*, 3476–3483.
[27] S. Fernandez, J. L. Mesa, J. L. Pizarro, L. Lezama, M. I. Arriortua, T. Rojo, *Chem. Mater.* **2003**, *15*, 1204–1209.
[28] G. Bonavia, J. DeBor, R. C. Haushalter, D. Rose, J. Zubieta, *Chem. Mater.* **1995**, *7*, 1995–1998.
[29] S. Fernandez, J. L. Mesa, J. L. Pizarro, L. Lezama, M. I. Arriortua, R. Olazcuaga, T. Rojo, *Chem. Mater.* **2000**, *12*, 2092–2098.
[30] S. Fernandez, J. L. Mesa, J. L. Pizarro, L. Lezama, M. I. Arriortua, T. Rojo, *Chem. Mater.* **2002**, *14*, 2300–2307.
[31] J. Durand, M. Loukili, N. Tijani, M. Wiq, L. Cot, *Eur. J.Solid State Inorg. Chem.* **1988**, *25*, 297.
[32] G. Férey, *J. Solid State Chem.* **2000**, *152*, 37–48.
[33] G. Férey, C. Mellot-Draznieks, T. Loiseau, *Solid State Sci.* **2003**, *5*, 79–94.
[34] R. L. Carlin, *Magneto-Chemistry*, Springer-Verlag, New York, **1986**.
[35] W. K. Chang, R. K. Chiang, Y. C. Jiang, S. L. Wang, S. F. Lee, K. H. Lii, *Inorg. Chem.* **2004**, *43*, 2564–2568.
[36] G. M. Sheldrick, *SHELXTL Programs*, Release Version 5.1, Bruker AXS, Madison, WI, **1998**.

Received: July 23, 2004

